

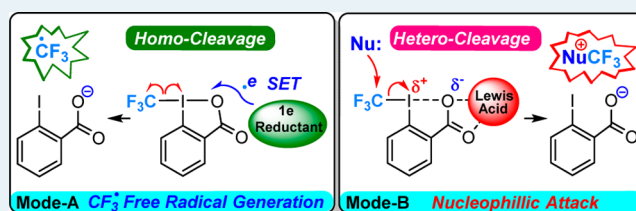
General Reaction Mode of Hypervalent Iodine Trifluoromethylation Reagent: A Density Functional Theory Study

Lin Ling,[†] Kun Liu,[‡] Xinqian Li,[†] and Yuxue Li*[†][†]State Key Laboratory of Organometallic Chemistry, Shanghai Institute of Organic Chemistry, Chinese Academy of Sciences, 345 Lingling Road, Shanghai 200032, P. R. China[‡]College of Chemistry, Tianjin Normal University, Tianjin 300387, P. R. China

Supporting Information

ABSTRACT: The mechanisms of trifluoromethylation with hypervalent iodine trifluoromethylation reagent (Togni's reagent **1**) have been comprehensively studied by density functional theory (DFT) calculations. The results show that there are two general reaction modes for reagent **1**: (I) **Mode-A**, acting as a CF₃[•] free radical source. When one-electron reductants are available in the reaction system, such as Cu^I, Fe^{II}, TEMPONa, or electron-rich lithium enolate, **1** will be reduced via single-electron transfer (SET) and give out CF₃[•] free radical concertedly. In the Cu^I-catalyzed trifluoromethylation of terminal olefins, Cu^I promotes the *homo*-cleavage of the F₃C–I bond in **1** via SET to produce Cu^{II} species and CF₃[•] free radical. Then the CF₃[•] free radical attacks the olefin, leading to trifluoromethyl alkyl radical intermediate. Subsequently, the Cu^{II} species act as a one-electron oxidant oxidizing the alkyl radical to carbocation intermediate, and the following deprotonation leads to the final product. Other mechanisms, such as formation of F₃C–Cu^{III} species via oxidative addition, formation of allylic radical intermediate, were considered and excluded. (II) **Mode-B**, acting as a CF₃⁺ cation source. **1** can be activated by a Lewis acid such as Zn^{II} and becomes more inclined to undergo an S_N2 type nucleophilic attack at the CF₃ group by nucleophiles (pentanol in this work). For substrates studied in this paper, such as the lithium enolate, pentanol, and sodium 2,4,6-trimethylphenolate, the competition between their reducibility and nucleophilicity determines the reaction mode of reagent **1**.

KEYWORDS: trifluoromethylation, Togni's reagent **1**, CF₃[•] radical, reaction mechanism, DFT, MECP, SET



INTRODUCTION

Trifluoromethylation is of great significance due to the wide application of molecules bearing trifluoromethyl groups in pharmaceutical chemistry, agrochemistry, and materials science.¹ Many efforts have been made to introduce the trifluoromethyl group into organic molecules.² In the past few years, the scope of trifluoromethylation reactions has been greatly expanded by electrophilic trifluoromethylating reagents developed by Umemoto³ and Togni^{4,5} et al. (Scheme 1A). Nowadays, numerous studies on trifluoromethylation using Togni's reagent have been published.^{2,6–13} However, despite that various mechanisms have been proposed on the basis of abundant experimental observations, the exact reaction pathways are still unidentified (Scheme 2). Under this condition, related theoretical investigations have been warranted for a long time. Herein we report a comprehensive density functional theory (DFT) study focusing on trifluoromethylation reactions using the hypervalent iodine trifluoromethylation reagent **1** (1-(trifluoromethyl)-1,2-benziodoxol-3(1H)-one). To obtain some generalities, several representative trifluoromethylation reactions were considered (Scheme 1B). Undoubtedly, it is impossible to exhaust all type of reactions and reagents in just one paper.

In 2011, several groups made breakthroughs in the direct allylic trifluoromethylation of unactivated terminal olefins

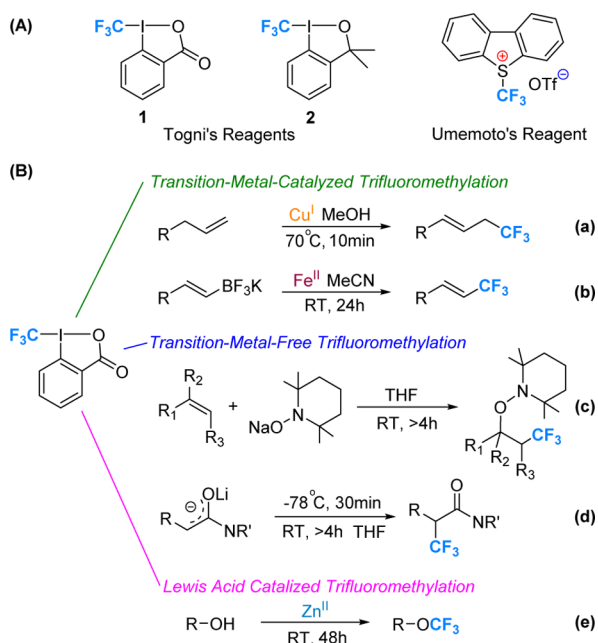
independently. Buchwald et al. reported this reaction using [Cu(MeCN)₄]PF₆ and **1** in methanol.^{6a} Liu and co-workers fulfilled this reaction with CuTc and Umemoto's reagent.^{14a} Wang et al. accomplished this reaction with **1** and CuCl (10 mol %) catalyst (Scheme 1, Reaction (a)).^{6b} Besides Cu^I, Fe^{II} also works in this type of reaction (Reaction (b)).^{7b} Thereafter, with **1**, trifluoromethylation of allylsilanes^{6c,d} and olefinic trifluoromethylations⁷ have been achieved. Meanwhile, difunctionalization of alkenes including *oxy*-,⁸ *amino*-,⁹ *carbo*-¹⁰ trifluoromethylations, and formation of F₃C–X (X = O, C, N, P and S)^{11–13} bonds with nucleophiles have been reported. Among these works, except “transition-metal-catalyzed” reaction, “transition-metal-free” trifluoromethylation of alkenes was reported by Studer et al. (Reaction (c)).^{8b,10d,k} As an electrophilic trifluoromethylating reagent, **1** shows reactivity toward nucleophiles to transfer a CF₃⁺ unit.^{13a,c} The trifluoromethylation of enolate to afford α -CF₃-substituted carbonyl compounds (Reaction (d))^{11b} and the trifluoromethylation of alcohols (Reaction (e)) were reported by Togni et al.^{12b}

Received: November 27, 2014

Revised: February 2, 2015

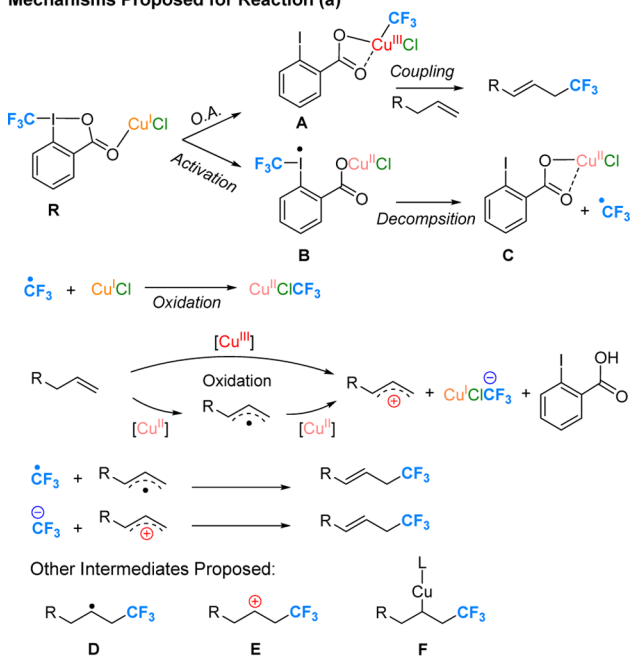
Published: March 10, 2015

Scheme 1. (A) Togni's Reagents and Umemoto's Reagent. (B) Trifluoromethylation Reactions Studied in This Work

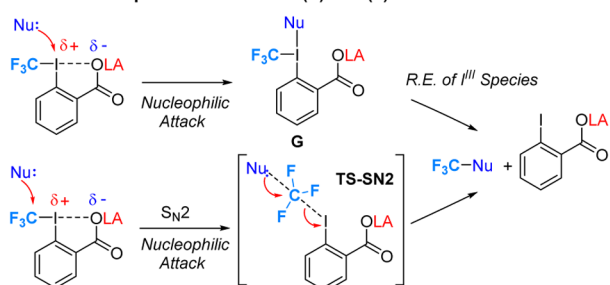


Scheme 2. Mechanisms Proposed for Reaction (a), (d), (e)

Mechanisms Proposed for Reaction (a)



Mechanisms Proposed for Reaction (d) and (e)



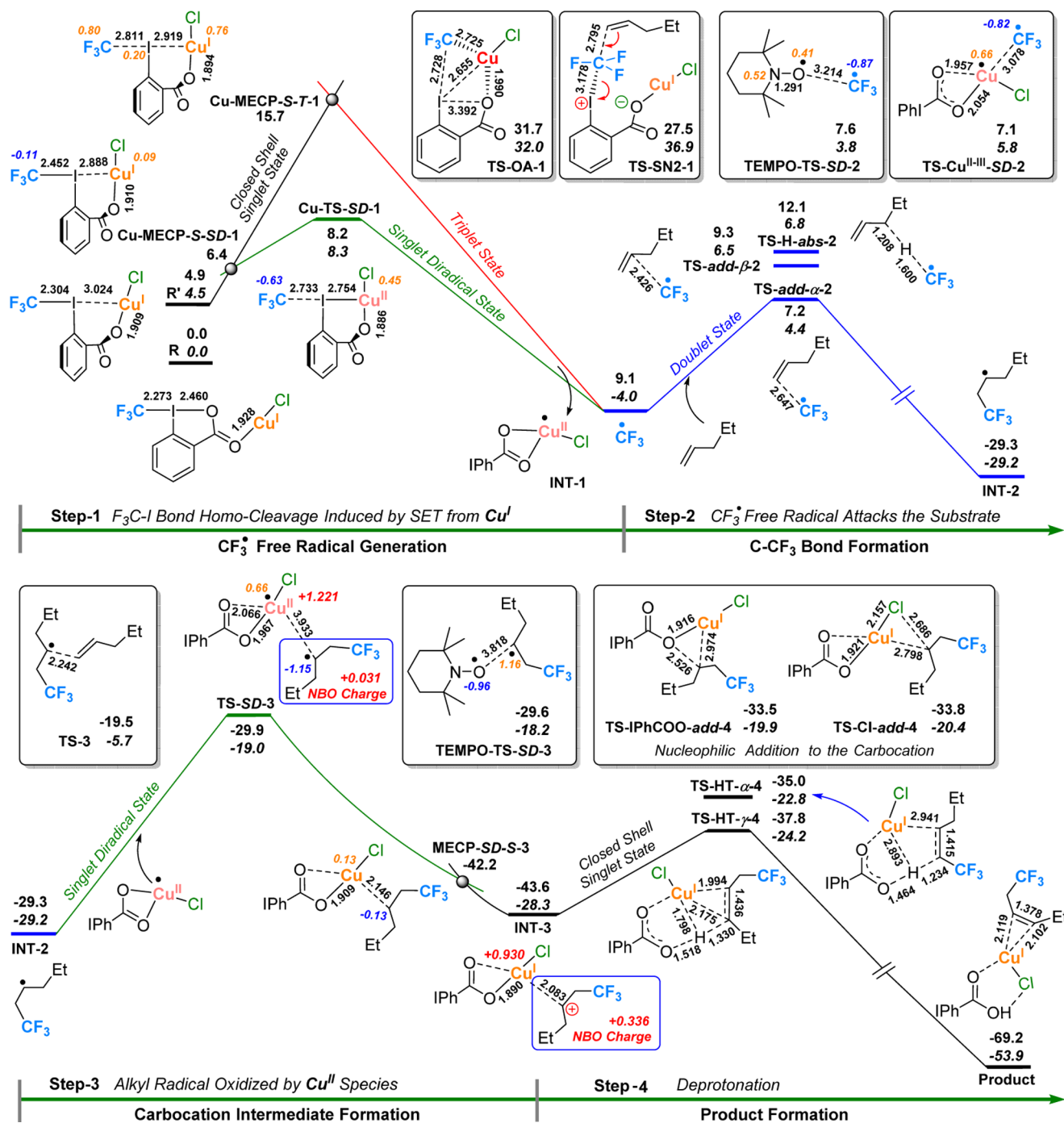
The mechanisms that have been proposed are indeed complicated (Scheme 2). For the trifluoromethylation of olefins (Reaction (a)), complex R may undergo a traditional oxidative addition (O.A.) yielding the $Cu^{III}-CF_3$ intermediate A, and subsequent coupling with olefin leads to the final product.^{6b} A Cu^{III} mechanism via a Heck-like four-membered-ring transition state has been reported in trifluoromethylation of olefins using Umemoto's reagent.^{14a} However, radical mechanisms are more often proposed.^{6a,b} The activation of Cu^I to 1 may first lead to CF_3 containing radical intermediate B, the decomposition of which generates the CF_3^\bullet free radical and the (2-iodobenzoyloxy) Cu^{II} chloride C. The catalyst $Cu^I Cl$ may be oxidized by the CF_3^\bullet free radical leading to the $Cu^{II} ClCF_3$ species. Subsequently, allylic radical and allylic cation may be generated via oxidation of the olefin substrate by Cu^{II}/Cu^{III} species. The combination of CF_3^\bullet free radical and the allylic radical, or the addition of CF_3^- anion to the allylic cation leads to the final product. In experiments using radical scavenger TEMPO (2,2,6,6-tetramethyl-1-piperidinyloxy) to probe the mechanism, reaction inhibition and TEMPO- CF_3 adduct were observed.^{6a,d,7d} In the test reaction with *alkenyl-cyclopropane* radical-clock substrate,^{6d} the ring opening trifluoromethylation product was detected. These observations support the generation of the CF_3^\bullet free radical. However, in the test reaction with *allylic-cyclopropane* radical-clock substrate,^{6a} a normal trifluoromethylation product was obtained, indicating that the formation of allylic radical intermediate may be unlikely. In addition, TEMPO-allyl adduct was not detected in Wang's experiment either.^{6b} Other intermediates, such as alkyl free radical D from an atom transfer radical addition to the C=C bond, cationic intermediate E from either electrophilic trifluoromethylation or oxidation of D, and alkyl-copper species F from D and the Cu catalyst, were also proposed.^{6a} For Reaction (c), the authors prefer a mechanism of in situ generation of TEMPO and CF_3^\bullet radicals, with TEMPO- CF_3 adduct as a minor product. For Reaction (d) and (e), two types of nucleophilic attack mechanisms were proposed. Under the activation of the Lewis acid, the nucleophile may attack the positively charged I atom to afford the new I^{III} intermediate G via "ligand exchange", and subsequent reductive elimination (R.E.) from the hypervalent iodine center affords the final product. Alternatively, the nucleophile may attack the CF_3 group directly in an S_N2 manner to form the product.

Thus, for trifluoromethylation with 1, the experimental observations are complicated and sometimes confusing. The proposed radical mechanisms are quite reasonable, at least for some cases. However, theoretical supports are rare. Very recently, a deep theoretical study on trifluoromethylation of acetonitrile with reagent 2 indicated that except for reductive elimination, an S_N2 nucleophilic attack is also possible.^{14d} As "electrophilic trifluoromethylating" reagent, the S_N2 mechanism is also expected for reagent 1, especially in reactions with nucleophiles. To date, the basic properties of 1, such as the barrier height to produce a CF_3^\bullet free radical is unknown. To make the mechanisms clear, in this paper, all the mechanisms proposed in Scheme 2 were tested by DFT calculations based on reactions listed in Scheme 1. A deep understanding and a clear description of the reaction pathways were given.

■ **MODELS AND METHODS**

To disclose the reaction mechanisms, density functional theory (DFT)¹⁵ studies have been performed with the Gaussian 09 program¹⁶ using the B3LYP¹⁷ method. For transition metals

Scheme 3. Calculated Pathways of Trifluoromethylation of Olefin with **1** and CuCl Catalyst^a; Step-1: CF₃• Free Radical Generation; Step-2: CF₃• Free Radical Attacks the Olefin Double Bond; Step-3: Alkyl Free Radical Oxidized to Carbocation by Cu^{II} Species; Step-4: Deprotonation of the Carbocation Intermediate



^aThe relative energies (ΔE_{sol} , in bold) and relative free energies (ΔG_{sol} , in bold italic) in methanol are given in kcal/mol. The selected bond lengths are in Å. The small orange and blue numbers are positive and negative spin densities, respectively. Selected NBO charges are given in red numbers. Calculated at the B3LYP/6-31+G**/SDD/Aug-cc-PVTZ level.

Cu, Fe, and Zn, the Aug-cc-PVTZ basis set was used; for the I atom, the SDD¹⁸ basis set with Effective Core Potential (ECP) was used; and for other atoms (C, H, O, N, B, F, Cl, S, Li, Na, K), the 6-31+G** basis set was used. Structures were optimized with the SMD¹⁹ method in solvents used in the experiments, as listed in Scheme 1. Harmonic vibration frequency calculations (298 K, 1 atm) confirmed the optimized stationary points are

either minima (having no imaginary vibration) or transition states (having one imaginary vibration).

In this study, the single-electron reduction/oxidation and the radical combination processes are all two-state reactions (TSR), which are attracting increasing attention from chemists.²⁰ For a two-state reaction, the minimum energy crossing point (MECP) between potential energy surface (PES) of different spin states must be located to calculate the reaction barrier. In

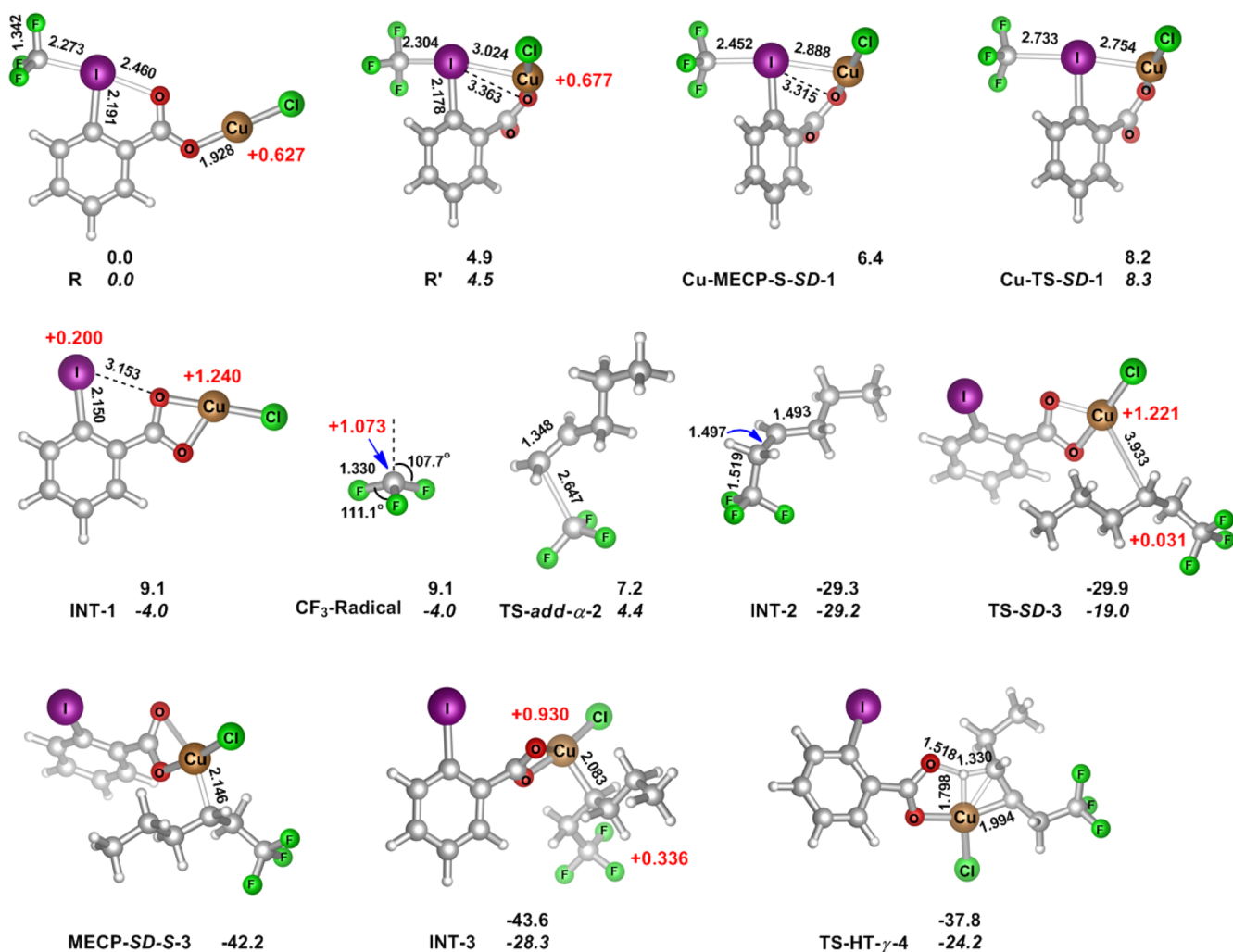


Figure 1. Selected optimized structures on pathways shown in Scheme 3 with selected bond lengths (in Å) and NBO atomic charges (in red). The relative free energies in methanol ΔG_{sol} are in kcal/mol. Calculated at B3LYP/6-31+G**/SDD/Aug-cc-PVTZ level.

the present work, the MECPs were located with the code developed by Harvey and co-workers.²¹ In organometallic chemistry, B3LYP is widely used in two-state mechanistic studies.²² In addition, for the *open-shell-singlet-diradical* system, the *broken symmetry* solution of B3LYP method was proved to be reasonable.²³ Further test calculations of *homo-cleavage* of the F₃C–I bond in CF₃I molecule show that B3LYP produces similar results with the CCSD(T) method.²⁴

RESULTS AND DISCUSSION

PART I. Reaction Mode-A: 1 Acts as a CF₃[•] Free Radical Source. Reaction (a): Trifluoromethylation of Terminal Olefins with 1 and CuCl Catalyst. In this part, the mechanisms of trifluoromethylation of terminal olefins with 1 and CuCl catalyst^{6b} have been studied intensively. However, to make clear and make sense, only the most favorable pathways and selected transition states of the competitive pathways are shown in Scheme 3. The selected optimized structures are shown in Figure 1. Some steps such as low barrier conformational changes are omitted. The complete pathways are collected in Supporting Information.²⁴ In the calculation, pentene was used as the olefin substrate.

Step-1: 1 Catalyzed by CuCl to Generate CF₃[•] Free Radical and Cu^{II} Species. As shown in Scheme 3, R is the reactant

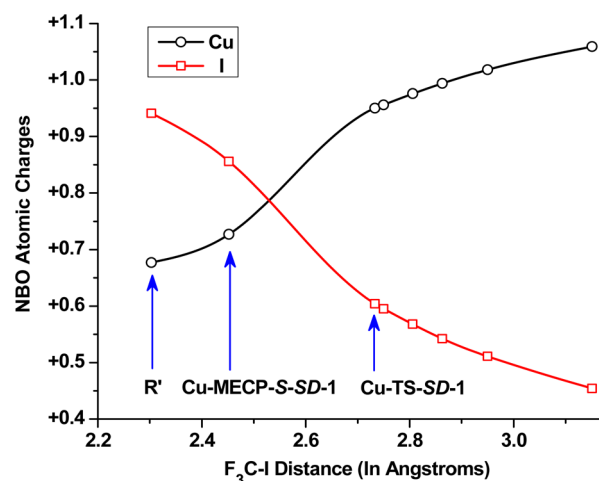
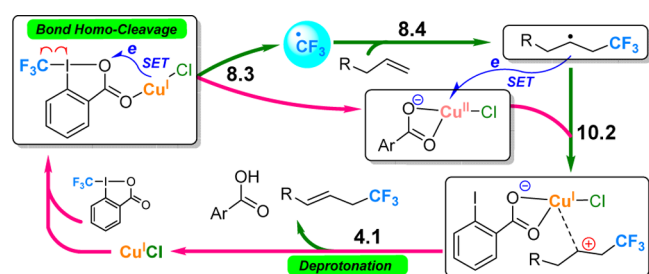


Figure 2. Variation of the NBO atomic charges on I and Cu atoms during the CF₃[•] free radical formation. The structures on the right side of the transition state (Cu-TS-SD-1) were obtained from IRC calculation.

complex of 1 and the CuCl catalyst. The oxidative addition pathway of 1 with Cu^ICl to generate Cu^{III}–CF₃ species was calculated (TS-OA-1, 32.0 kcal/mol).²⁴ The barrier is too high

Scheme 4. Pathway of Trifluoromethylation of Terminal Olefins with **1** and CuCl Catalyst^a

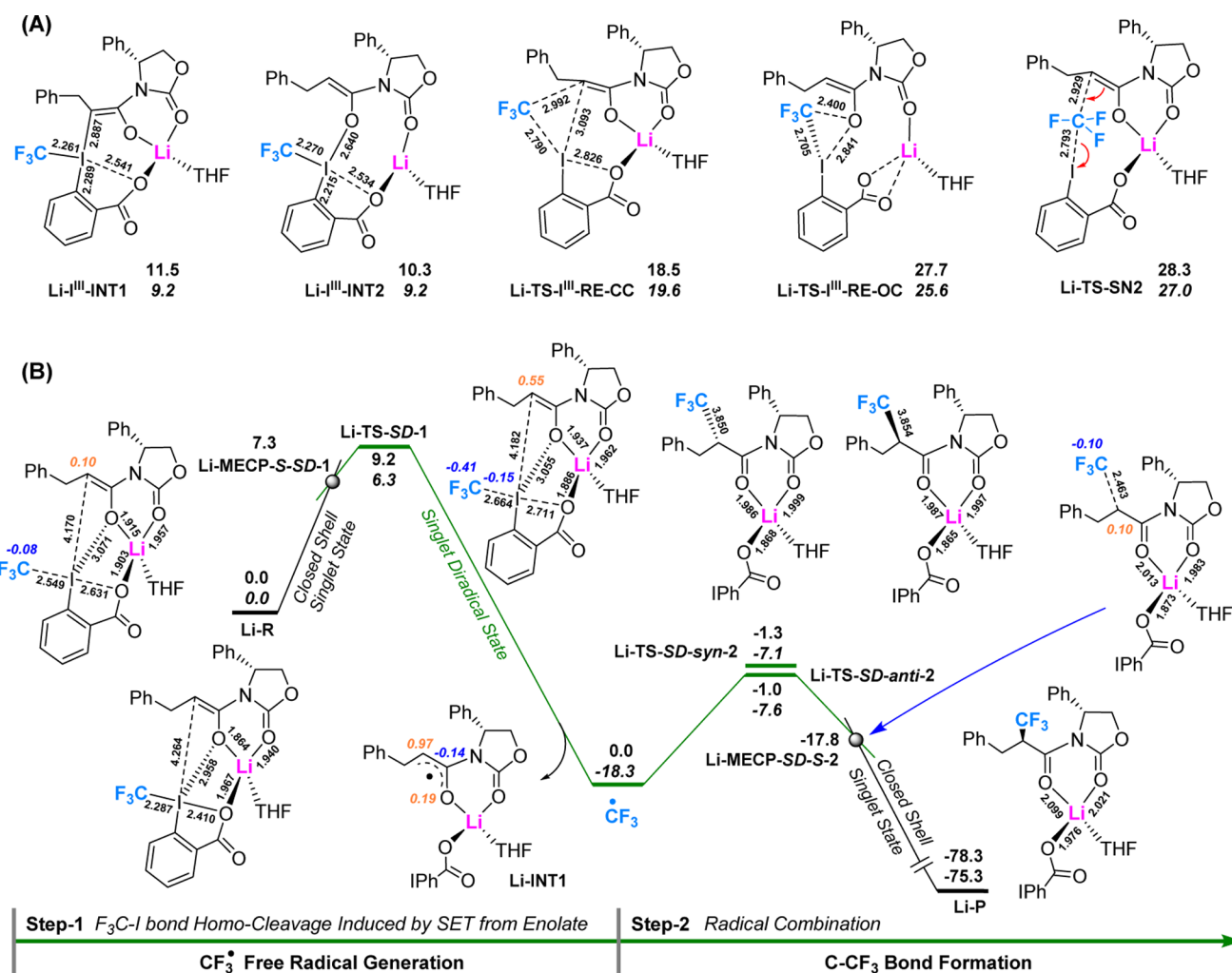
^aThe numbers are free energy barriers of each step.

to be reasonable under the experimental conditions. However, it should be noted that in experiments using electron-rich ligands, this mechanism cannot be excluded because the Cu^{III}–CF₃ species can be stabilized greatly by the ligand used.^{14a} In TS-SN2–1, **1** acts as a CF₃⁺ source. Because the alkene is not a good nucleophile, the barrier of this S_N2 attack is very high (36.9 kcal/mol). Furthermore, our calculations also indicate that the “CF₃-containing radical intermediate” **B** (Scheme 2) is

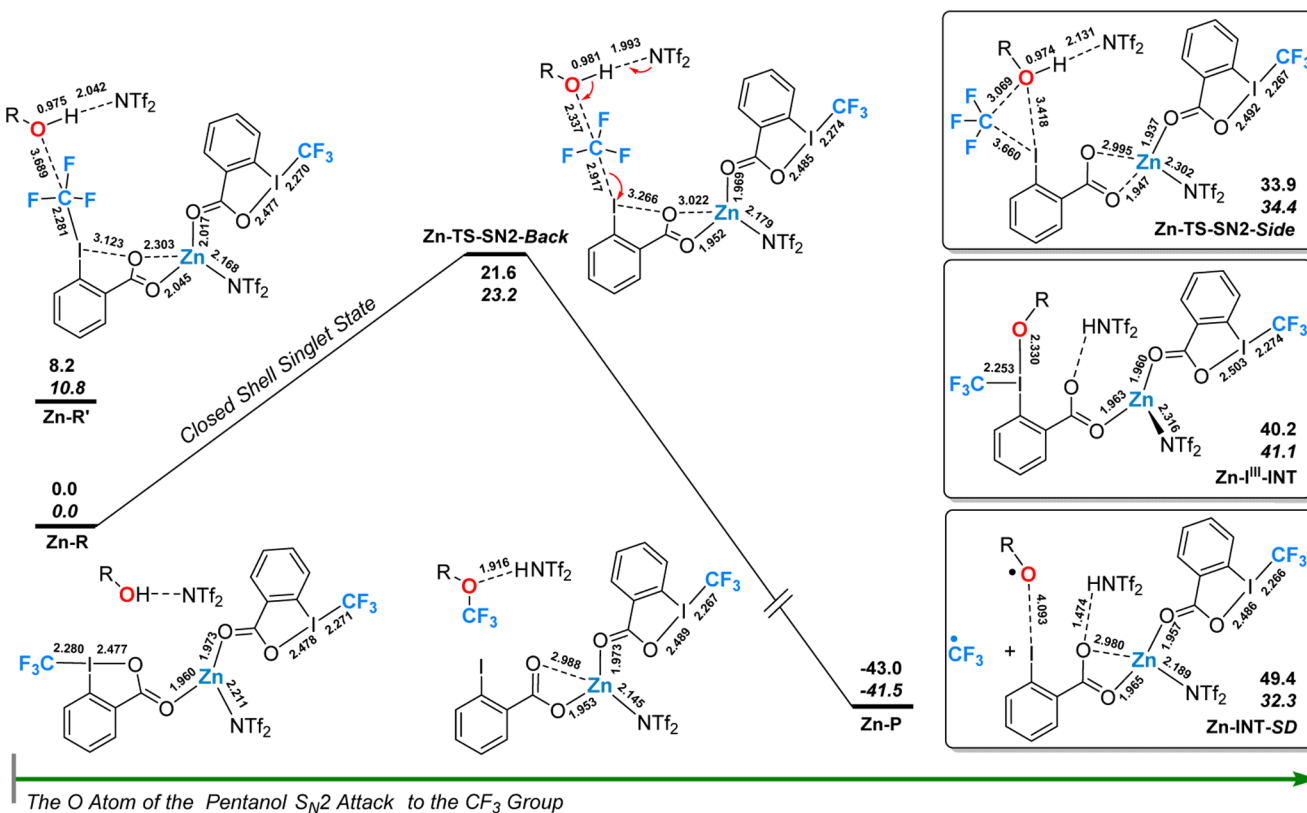
not a local minimum on both the *triplet* and the *singlet-diradical* state potential energy surfaces.²⁴

R' is a more reactive configuration in which the I–O bond breaks (3.363 Å), and the catalyst Cu^I weakly coordinates with the I atom. There are two pathways to generate CF₃[•] free radical via spin inversion through the minimum energy crossing points (MECPs). On the favorable pathway, through Cu-MECP-S-SD-1 (6.4 kcal/mol), **R'** crosses to the *singlet-diradical* (SD) potential energy surface and then crosses over transition state Cu-TS-SD-1 (8.3 kcal/mol), leading to the CF₃[•] free radical and the Cu^{II} species INT-1 (**C** in Scheme 2). Direct generation of CF₃[•] free radical from **R** needs to overcome a higher barrier (14.4 kcal/mol).²⁴ The pathway via the *closed-shell-singlet* state and *triplet* state MECP Cu-MECP-S-T-1 (15.7 kcal/mol) is less favorable.

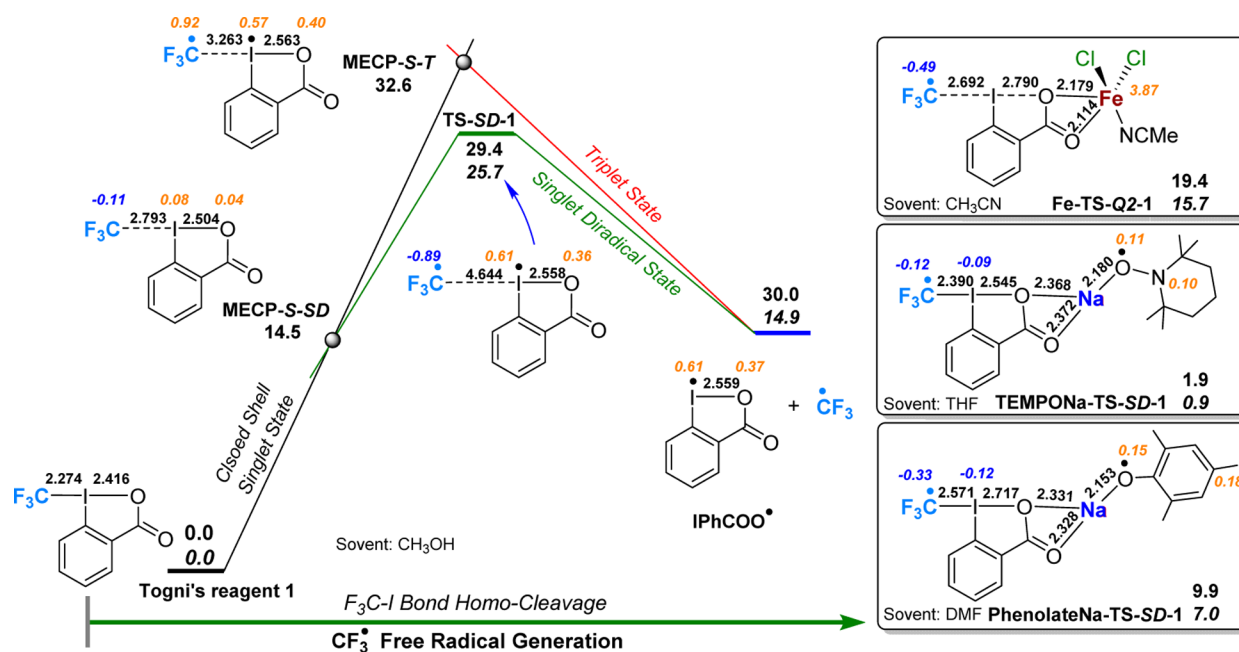
In **R'**, the F₃C–I bond is 2.304 Å and increases to 2.733 Å in Cu-TS-SD-1, in which there are –0.63 spin density on the carbon atom of the CF₃ group and +0.45 spin density on the copper atom. This indicates that the homolytic bond cleavage is concerted with the SET process. Figure 2 shows the variation of the NBO²⁵ atomic charges on I and Cu atoms during the CF₃[•] free radical formation. It demonstrates that the increasing of the

Scheme 5. Calculated Pathways of C-Trifluoromethylation of Enolate with **1**^a

^aThe relative energies (ΔE_{sol} in bold) and relative free energies (ΔG_{sol} in bold italic) in THF are in kcal/mol. The selected bond lengths are in Å. Orange and blue numbers are positive and negative spin densities. Calculated at the B3LYP/6-31+G**/SDD level.

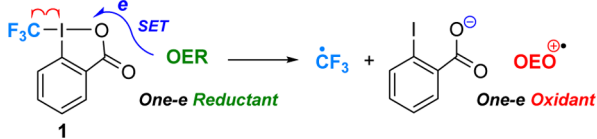
Scheme 6. Calculated Trifluoromethylation Pathways of Pentanol with **1** and Zn(NTf₂)₂ Catalyst^a

^aThe relative energies (ΔE_{sol} in bold) and the relative free energies in 1-pentanol (ΔG_{sol} in bold italic) were given in kcal/mol. The selected bond lengths are in Å. NBO charges are given. Calculated at the B3LYP/6-31+G**/SDD/Aug-cc-PVTZ level.

Scheme 7. Calculated Pathways of **1** to Produce a CF₃[•] Free Radical without Catalyst^a

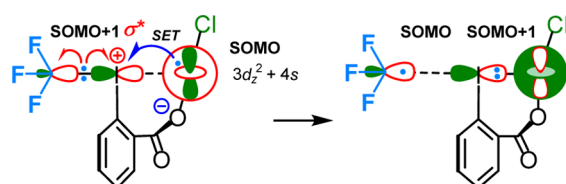
^aThe key transition states of the Fe^{II}-catalyzed process and the key transition states of TEMPONa and PhenolateNa React with **1** are also given. The relative energies in solvent (ΔE_{sol} in bold) and the relative free energies in solvent (ΔG_{sol} in bold italic) were given in kcal/mol. The selected bond lengths are in Å. Orange and blue numbers are positive and negative spin densities. Calculated at the B3LYP/6-31+G**/SDD/Aug-cc-PVTZ level.

Table 1. Calculated Reaction Barrier and Gibbs Free Energy Change (in kcal/mol) for 1 To Produce a CF₃• Free Radical under Different Conditions



OER (one-electron reductant)	barrier to produce radical	CF ₃ • free radical	ΔG of the reaction
none	25.7		14.9
Cu ^I	8.3		-4.0
Fe ^{II}	15.7		-3.9
enolateLi	6.3		-18.3
TEMPONa	0.9		-55.1
pentanol	>32.3		32.3
2,4,6-trimethylphenolateNa	7.0		-21.8

Scheme 8. Qualitative Understanding of the Orbital Interactions in CF₃• Free Radical Generation Process



positive charges on Cu atom is accompanied by the decreasing of the positive charges on I atom, clearly indicating that the electron is transferring from Cu atom to I atom in this process.

Experiments show that the CF₃• free radical generation step is fast. When 1 was added, the colorless CuCl solvent turned at once to blue-green, which is a feature of Cu^{II} ion.^{2f} Because the generation of the CF₃• free radical does not depend on the alkene substrate, it is natural that TEMPO–CF₃ adduct can be formed under standard conditions in the absence of the alkene.^{6b,24}

Step-2: CF₃• Free Radical Attacks the Olefin Double Bond. As shown in **Step-2** in Scheme 3, the CF₃• free radical directly

attacks the terminal carbon of the double bond via transition state **TS-add-α-2** over a barrier of 8.4 kcal/mol, leading to alkyl radical **INT-2** (**D** in Scheme 2). The formation of alkyl radical species is partially supported by the reaction with diethyl diallylmalonate as a cyclization radical-clock in Buchwald's work.^{6a} The barrier of CF₃• free radical attacking the β-carbon of the double bond (**TS-add-β-2**) to yield branched product is less favorable by 2.1 kcal/mol. As shown in Figure 1, there are large positive NBO atomic charges (+1.073) on the central carbon of the CF₃• free radical. Therefore, the preference of **TS-add-α-2** may result from the electrophilic nature of CF₃• free radical and the larger electronic density on α carbon than on β carbon in free pentene (NBO atomic charge: -0.489 vs -0.215).

The barrier to oxidize Cu^I complex by CF₃• free radical leading to Cu^{II}–CF₃ species is 10.3 kcal/mol,²⁴ which is 1.9 kcal/mol less favorable than **TS-add-α-2**. The barrier to oxidize Cu^{II} complex by CF₃• free radical (**TS-Cu^{II-III}-SD-2**) to afford Cu^{III}–CF₃ species is 9.8 kcal/mol, which is much lower than that of the direct oxidation pathway (**TS-OA-1**, 32.0 kcal/mol). However, it is still 1.4 kcal/mol less favorable than **TS-add-α-2**, and the subsequent Cu^{III} pathways are also less favorable.²⁴

The H-abstraction transition state **TS-H-abs-2** which yields allylic radical intermediate is 2.4 kcal/mol less favorable than **TS-add-α-2**. Additionally, calculations show that the generation of allylic radical via oxidation of olefin by Cu^{II} species is endergonic by 18.4 kcal/mol, indicating that the barrier must be even higher.²⁴ Therefore, the possibility to generate the allylic radical is unlikely. This is consistent with the experimental results showing that *allylic-cyclopropane* substrate gives normal product^{6a} and that no TEMPO-allyl adduct was detected.^{6b}

The barrier of CF₃• free radical to be captured by the well-known radical scavenger 2,2,6,6-tetramethyl-1-piperidinyloxy (TEMPO) is 0.6 kcal/mol more favorable than **TS-add-α-2**, indicating that CF₃• free radical reacts faster with TEMPO than with the terminal olefins. However, the barrier gap is small. Therefore, both pathways should be accessible. This result is consistent with the experimental observations in Wang's work.^{6b} When 1.75 equiv of TEMPO was added in the reaction system, most of the CF₃• free radicals were trapped by

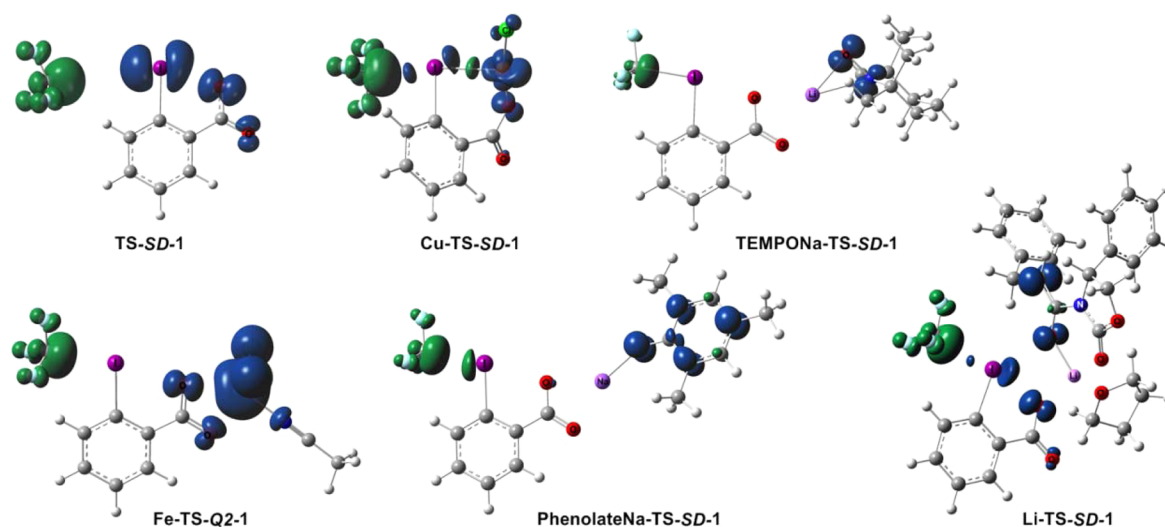


Figure 3. Spin densities of **TS-SD-1**, **Cu-TS-SD-1**, **TEMPONa-TS-SD-1**, **Fe-TS-Q2-1**, **PhenolateNa-TS-SD-1**, and **Li-TS-SD-1**. Depicted using isodensity at 0.004 au. Negative and positive spin densities are shown in green and blue, respectively.

TEMPO leading to TEMPO-CF₃ (79%); meanwhile, 1% normal trifluoromethylation product was obtained.

Step-3: Oxidation of the Alkyl Radical Intermediate to Carbocation Intermediate by Cu^{II} Species. As shown in Step-3 in Scheme 3, INT-2 binds with the Cu^{II} complex, walks along the singlet-diradical state potential energy surface (PES), overcomes a barrier of 10.2 kcal/mol (TS-SD-3), then passes through MECP-SD-S-3 and leads to INT-3 (E in Scheme 2). The pathway via the triplet/closed-shell-singlet MECP (-27.0 kcal/mol) is less favorable and not shown here.^{24,26} As shown in Figure 1, in transition state TS-SD-3, the Cu-C distance is 3.933 Å, and the NBO atomic charge on the Cu center is +1.221, which is close to that of the Cu^{II} species INT-1 (+1.240). The NBO charge on the whole alkyl group is very small (+0.031), being nearly neutral. In INT-3, the Cu-C distance is 2.083 Å with a Wiberg bond index of 0.5743, the NBO atomic charges on the Cu center decrease to +0.930, and the NBO charges on the whole alkyl group increase to +0.336. These results indicate that the electrons transfer from the alkyl radical group to the Cu^{II} center. Thus, in INT-3, the alkyl group becomes a carbocation, and the copper is in formal Cu^I oxidation state. Inspection of the molecule orbital (MO) shows that this C-Cu bond is mainly contributed by the back-donation from 4s and 3d atomic orbitals of Cu^I center to the empty 2p atomic orbital of the carbocation.²⁴

Why has the theoretically predicted alkyl radical intermediate INT-2 not been trapped by TEMPO in the experiment? Our calculations show that INT-2 is more readily oxidized by Cu^{II} species (TS-SD-3, -19.0 kcal/mol) leading to the normal trifluoromethylation product than reacting with TEMPO (TEMPO-TS-SD-3, -18.2 kcal/mol). In addition, when most of the CF₃• free radicals were trapped by TEMPO, only a small amount of alkyl radical intermediate could be formed.

The barrier of the alkyl radical intermediate INT-2 attacking a second molecule of olefin (TS-3, -5.7 kcal/mol) is much less favorable, showing that the olefin polymerization is unlikely. Furthermore, the reaction of INT-2 with Cu^I to produce alkyl-copper species F is both kinetically and thermodynamically less favorable.²⁴

Step-4: Deprotonation of the Carbocation Intermediate To Form the Final Product. For the carbocation intermediate INT-3, in the deprotonation process, transition state TS-HT-γ-4, which leads to allylic trifluoromethylation product, is 1.4 kcal/mol more favorable than TS-HT-α-4, which leads to olefinic trifluoromethylation product. In TS-HT-γ-4, the C-H bond is activated by the Cu center,²⁴ which is indicated by the short H...Cu distance of 1.798 Å. This is similar to the cyclometalation catalyzed by palladium acetate.²⁷ The barriers to eliminate α-H and γ-H of INT-3 are close, indicating that under certain conditions, the elimination of the α-H is also possible. When a substrate without an allylic proton, such as styrene, is used, the elimination of the α-H is the only choice, and the trifluoromethyl-substituted alkene is obtained.⁷¹ The regioselectivity of the elimination can be controlled by using better leaving groups, such as BF₃K in potassium vinyl-trifluoroborates. In trifluoromethylation of allylsilanes, the silyl group can be eliminated.

Naturally, the carbocation intermediate INT-3 may undergo nucleophilic attack by nucleophiles such as the coordinated Cl⁻ or *o*-IPhCOO⁻ anion. The calculated results show that the barriers of Cl⁻ and *o*-IPhCOO⁻ addition to the carbocation are 3.8 and 4.3 kcal/mol higher than that of the deprotonation process, respectively (TS-Cl-add-4 and TS-IPhCOO-add-4).

This is well consistent with the fact that no nucleophilic attack product was detected in this experiment. However, the small barrier gap of about 4 kcal/mol indicates that under certain conditions, the trifluoromethylation/nucleophilic-addition difunctionalization product may be formed. In fact, the Cl⁻ anion addition trifluoromethylation product (15%) was actually observed by Buchwald.^{6a,7b} The *o*-IPhCOO⁻ anion addition trifluoromethylation of styrene was obtained in Szabó and Sodeoka's works,^{8c,d} and when base was added to facilitate the deprotonation, trifluoromethylated alkenes could be obtained.⁷¹

We propose that in trifluoromethylation of alkenes with **1** and transition metal as one-electron reductant/oxidant, the carbocation intermediate may be formed in many cases. With this notion, mechanisms of many difunctionalization reactions of alkenes could be understood based on the carbocation chemistry, such as trapped by nucleophiles and intramolecular Friedel-Crafts type reaction.⁸⁻¹⁰ To show the mechanisms more clearly, a summary of the whole reaction pathway is given in Scheme 4.

Reaction (d): α-Trifluoromethylation of Evans-Type Chiral Lithium Imide Enolate with 1. As for the synthesis of α-CF₃-substituted carbonyl compounds using lithium imide enolates and **1**,^{11b} in the originally proposed pathways, new I^{III} intermediate (G in Scheme 2) is formed via nucleophilic attack to the I atom by the carbanion, and subsequent reductive elimination from the I^{III} center affords the final product. As shown in Scheme 5A, we located the I^{III} intermediates Li-I^{III}-INT1 (9.2 kcal/mol) with a newly formed weak C-I bond (2.887 Å) and Li-I^{III}-INT2 (9.2 kcal/mol) with a newly formed weak O-I bond (2.640 Å). The overall barrier of reductive elimination of Li-I^{III}-INT1 to afford the final product is 19.6 kcal/mol (Li-TS-I^{III}-RE-CC), which seems quite reasonable. The reductive elimination transition state Li-TS-I^{III}-RE-OC (25.6 kcal/mol) from Li-I^{III}-INT2 to afford *O*-trifluoromethylation product, and the S_N2 nucleophilic attack transition state Li-TS-SN2 (27.0 kcal/mol) were also located. They are both less favorable.

However, besides being good nucleophiles, enolates are reductants, and they can be oxidized under mild conditions by the ferrocenium ion [FeCp₂]⁺, a mild one-electron oxidant.²⁸ Therefore, the radical mechanism must be considered. As shown in Scheme 5B, via Li-TS-SD-1 (6.3 kcal/mol), the CF₃• free radical generated concertedly with the oxidation of the enolate to α-carbonyl radical (Li-INT1), in which large spin (0.97) distributes on the β-carbon. The barrier of the CF₃• free radical generation is much lower than that of the reductive elimination of Li-I^{III}-INT1. Subsequently, the combination of the CF₃• free radical with the α-carbonyl radical passes over transition state Li-TS-SD-anti-2 (-7.6 kcal/mol), leading to the final product. Transition state Li-TS-SD-syn-2 is 0.5 kcal/mol less favorable, which is qualitatively consistent with the product selectivity in the experiments.^{11b} To avoid steric interactions, the CF₃• free radical favors to attack the α-carbonyl radical from the anti-side of the phenyl group on the five-membered ring. Thus, the enolate acts as a one-electron reductant, rather than a nucleophile. It is reasonable for being consistent with the mechanisms proposed in previous experiments.²⁹

Part II. Reaction Mode-B: 1 Acts as a CF₃⁺ Source.
Reaction (e): *O*-Trifluoromethylation of Pentanol with 1 and Zn(NTf₂)₂ Catalyst. **1** is able to trifluoromethylate of certain nucleophiles.^{13a,c} In this part, the mechanisms of *O*-trifluoromethylation of pentanol with **1** and Zn(NTf₂)₂ catalyst

to afford trifluoromethyl ether^{12b} have been studied (Scheme 6). ESI-MS spectrum shows that the zinc dicarboxylate complex $[\text{Zn}^{\text{II}}(\mathbf{1})_2(\text{NTf}_2)]^+$ is the main species in the reaction system.^{12b} Therefore, the adduct of one Zn^{II} with two $\mathbf{1}$ was used as the reactant complex (**Zn-R**). The NTf_2^- anion forms hydrogen bonding with the hydroxyl group, increasing the nucleophilicity of the hydroxyl O atom. In transition state **Zn-TS-SN2-Back**, the pentanol O atom attacks the CF_3 group backside in an $\text{S}_{\text{N}}2$ manner assisted by the NTf_2^- anion to accept the proton, crossing over a barrier of 23.2 kcal/mol leading to the trifluoromethylation product **Zn-P**. The *side*-attack transition state **Zn-TS-SN2-Side** is 11.2 kcal/mol less favorable. **Zn-R'** is a configuration in which the I–O bond breaks. This structure leads to a slightly higher transition state **Zn-TS-SN2-Back'** (24.5 kcal/mol).²⁴ To test the I^{III} reductive elimination mechanism, the intermediate **Zn-I^{III}-INT** was located. Its relative free energy is 41.1 kcal/mol, indicating that the reductive elimination mechanism is impossible. The free energy change for CF_3^\bullet free radical generation is 32.3 kcal/mol (**Zn-INT-SD**), which is even higher than the CF_3^\bullet free radical generation of $\mathbf{1}$ without catalyst (25.7 kcal/mol, Scheme 7). Therefore, the radical mechanism can be excluded safely.

Based on the mechanistic studies on Reaction (d) and (e), we propose that, in these cases, the selectivity of the reaction mode of $\mathbf{1}$ depends on the competition of the nucleophilicity and the reducibility of the substrate. In Reaction (d), the lithium enolate is a strong nucleophile. However, it is also a strong one-electron reductant due to its ability to delocalize the spin. The pentanol is a weak reductant, indicated by the highly unstable alkoxy radical species **Zn-INT-SD**. In the *O*-trifluoromethylation of phenols,^{12a,24} the trifluoromethylation occurred preferentially at the *para*-position of the aromatic ring, and the expected *O*-trifluoromethylation product is obtained only in lower yields. Our calculations show that the barrier of an $\text{S}_{\text{N}}2$ attack of the phenolate O atom to the CF_3 group is 33.3 kcal/mol, and the barrier of reductive elimination for an I^{III} intermediate is 27.5 kcal/mol. However, the barrier of the CF_3^\bullet free radical generation is 7.0 kcal/mol (Scheme 7 and Table 1). In addition, the product distribution observed in the experiment is consistent with the spin density distribution on the phenolate radical. These results show that the behavior of the sodium phenolate is similar to that of the lithium enolate, which is in return supporting the mechanisms proposed for Reaction (d).

Part III. The Nature of the CF_3^\bullet Free Radical Generation. To find out how the Cu^{I} catalyst promotes the generation of CF_3^\bullet free radical, the CF_3^\bullet free radical generation pathway without Cu^{I} catalyst was calculated (Scheme 7). The energy of the transition state **TS-SD-1** increases to 25.7 kcal/mol, and the Gibbs free energy change of the reaction increases to 14.9 kcal/mol, showing that without the Cu^{I} catalyst, this reaction is much less favorable both kinetically and thermodynamically. Further calculations show that the formation of CF_3^\bullet free radical and *o*- IPhCOO^- anion is much lower in free energy (26.2 kcal/mol) than the formation of CF_3^- anion and IPhCOO^\bullet free radical, indicating that IPhCOO^\bullet free radical is a very strong one-electron oxidant. Therefore, the difficulty for $\mathbf{1}$ itself to produce CF_3^\bullet free radical originates from the high instability of the concomitantly generated IPhCOO^\bullet free radical. Consequently, when a one-electron reductant, such as Cu^{I} , is available in the reaction, the highly unstable IPhCOO^\bullet free radical is reduced to stable *o*- IPhCOO^- anion via SET from the catalyst. It is this driving

force that makes the CF_3^\bullet free radical generation thermodynamically favorable. The reduction process is happening in the transition state **Cu-TS-SD-1** (Scheme 3) and coordinated with the elongation of the $\text{F}_3\text{C}-\text{I}$ bond (i.e., the generation of the CF_3^\bullet free radical). Therefore, the SET from the catalyst also lowers the reaction barrier. The heterolytic dissociation of $\mathbf{1}$ to give CF_3^+ cation or CF_3^- anion is thermodynamically less favorable (27.5 and 49.8 kcal/mol, respectively) and can be safely ruled out.²⁴

To have a deeper understanding of the mechanisms, the CF_3^\bullet free radical generation pathways of the Fe^{II} -catalyzed^{7b} (Reaction (b) in Scheme 1) and the “transition-metal-free” trifluoromethylation^{8b} (Reaction (c) in Scheme 1) were studied (Scheme 7 and Table 1). The results show that in the Fe^{II} -catalyzed reaction, the barrier to produce CF_3^\bullet free radical is 15.7 kcal/mol, and exergonic by -3.9 kcal/mol, which is consistent with the experimental conditions. When Fe^{III} was used in the reaction, only a small amount of product was obtained.^{7b} This fact supports the calculation results that Fe^{II} acts as a one-electron reductant rather than a Lewis acid. When TEMPONa reacts with $\mathbf{1}$, the TEMPO^- anion is very easy to be oxidized, and the barrier to produce CF_3^\bullet and TEMPO radicals is only 0.9 kcal/mol and exergonic by -55.1 kcal/mol. In this reaction, the CF_3^\bullet free radical is more ready to react with the styrene substrate than with TEMPO.²⁴

Based on an inspection of the molecule orbitals (MO), a qualitative understanding of the orbital interactions in the CuCl catalyzed CF_3^\bullet free radical generation process is proposed (Scheme 8). For **Cu-MECP-S-SD-1**, the singly occupied molecular orbital (SOMO) is mainly composed of $3d_{z^2}$ and $4s$ atomic orbitals of the Cu^{I} atom. The empty SOMO+1 is mainly composed of the $\text{F}_3\text{C}-\text{I}$ *anti*-bonding orbital. The SET from SOMO to SOMO+1, largely from the Cu^{I} atom to I^{III} atom, promotes the homolytic cleavage of the $\text{F}_3\text{C}-\text{I}$ σ bond. The I^{III} atom is reduced to I^{I} , concomitantly yields the CF_3^\bullet free radical and Cu^{II} species.

Figure 3 shows the spin densities of **TS-SD-1**, **Cu-TS-SD-1**, **TEMPONa-TS-SD-1**, **Fe-TS-Q2-1**, **PhenolateNa-TS-SD-1**, and **Li-TS-SD-1**. In **TS-SD-1**, the forming positive spin densities (in blue) are concentrated on the I and O atoms, to produce the highly unstable IPhCOO^\bullet free radical. However, in other transition states, the forming positive spin densities are mainly concentrated on the reductants.

CONCLUSION

In view of the importance of Togni's reagent $\mathbf{1}$ in trifluoromethylation, comprehensive mechanistic studies have been performed with DFT calculations. The results show that there are two general reaction modes for $\mathbf{1}$: acting as a CF_3^\bullet free radical source or a CF_3^+ cation source. In most cases, when one-electron reductants are available, $\mathbf{1}$ will be reduced via single-electron transfer (SET), producing CF_3^\bullet free radical and *o*- IPhCOO^- anion concertedly. In the Cu^{I} -catalyzed trifluoromethylation of terminal olefins, Cu^{I} assists *homo*-cleavage of the $\text{F}_3\text{C}-\text{I}$ bond in $\mathbf{1}$ via SET to produce Cu^{II} species and CF_3^\bullet free radical. Then the CF_3^\bullet free radical attacks the olefin, leading to trifluoromethyl alkyl radical intermediate. Subsequently, the Cu^{II} species act as a one-electron oxidant to oxidize the alkyl free radical to carbocation intermediate, and subsequent deprotonation leads to the final product. This study presents a better understanding on how fine-tuning of the experimental conditions and substrate modifications can lead to different products.

During the CF_3^\bullet free radical generation, the highly unstable IPhCOO^\bullet free radical is reduced to stable $o\text{-IPhCOO}^-$ anion via SET from the catalyst (or substrate). It is this driving force that makes the CF_3^\bullet free radical generation process both kinetically and thermodynamically favorable. The SET and the CF_3^\bullet free radical generation are concerted.

Lewis acid such as Zn^{2+} can activate **1** and make it more readily to undergo an $\text{S}_{\text{N}}2$ nucleophilic attack at the CF_3 group to give out a CF_3^+ cation moiety. For substrates such as lithium enolate and pentanol, the competition between their reducibility and nucleophilicity determines the reaction mode of **1**. Further mechanistic studies on other trifluoromethylating reagents are undertaken.

■ ASSOCIATED CONTENT

Supporting Information

The following file is available free of charge on the ACS Publications website at DOI: 10.1021/cs501892s.

The detailed reaction pathways, test calculations, selected molecular orbitals, and the calculated total energies and geometrical coordinates (PDF)

■ AUTHOR INFORMATION

Corresponding Author

*E-mail: liyuxue@sioc.ac.cn.

Notes

The authors declare no competing financial interest.

■ ACKNOWLEDGMENTS

This project is supported by the National Basic Research Program of China (973 Program, No. 2015CB856600) and the Natural Science Foundation of China (Grant Nos. 21402229, 21172173, 21172248, 21372249, 21421091).

■ REFERENCES

- (1) (a) Kirsch, P. *Modern Fluoroorganic Chemistry, Synthesis, Reactivity, Applications*; Wiley-VCH: Weinheim, 2004, pp 111–148. (b) Shimizu, M.; Hiyama, T. *Angew. Chem., Int. Ed.* **2005**, *44*, 214–231. (c) Müller, K.; Faeh, C.; Diederich, F. *Science* **2007**, *317*, 1881–1886.
- (2) For recent reviews, see (a) Ma, J.-A.; Cahard, D. *J. Fluorine Chem.* **2007**, *128*, 975–996. (b) Gawronski, J.; Wascinska, N.; Gajewy, J. *Chem. Rev.* **2008**, *108*, 5227–5252. (c) Kieltsch, I.; Eisenberger, P.; Stanek, K.; Togni, A. *Chimia* **2008**, *62*, 260–263. (d) Shibata, N.; Matsnev, A.; Cahard, D. *Beilstein J. Org. Chem.* **2010**, *6*, No. 65. (e) Merritt, E. A.; Olofsson, B. *Synthesis* **2011**, 517–538. (f) Wang, X.; Zhang, Y.; Wang, J. *Sci. Sin. Chim.* **2012**, *42*, 1417–1427. (g) Studer, A. *Angew. Chem., Int. Ed.* **2012**, *51*, 8950–8958. (h) Koike, T.; Akita, M. *J. Fluorine Chem.* **2014**, *167*, 30–36. (i) Egami, H.; Sodeoka, M. *Angew. Chem., Int. Ed.* **2014**, *53*, 8294–8308. (j) Xu, J.; Liu, X.; Fu, Y. *Tetrahedron Lett.* **2014**, *55*, 585–594. (k) Merino, E.; Nevado, C. *Chem. Soc. Rev.* **2014**, *43*, 6598–6608. (l) Liu, X.; Xu, C.; Wang, M.; Liu, Q. *Chem. Rev.* **2015**, *115*, 683–730.
- (3) (a) Umemoto, T.; Ishihara, S. *Tetrahedron Lett.* **1990**, *31*, 3579–3582. (b) Umemoto, T.; Ishihara, S. *J. Am. Chem. Soc.* **1993**, *115*, 2156–2164. (c) Umemoto, T. *Chem. Rev.* **1996**, *96*, 1757–1777.
- (4) For synthesis of Togni's reagent, see (a) Eisenberger, P.; Gischtig, S.; Togni, A. *Chem. - Eur. J.* **2006**, *12*, 2579–2586. (b) Matoušek, V.; Pietrasiak, E.; Schwenk, R.; Togni, A. *J. Org. Chem.* **2013**, *78*, 6763–6768. (c) Santschi, N.; Sarott, R. C.; Otth, E.; Kissner, R.; Togni, A. *Beilstein J. Org. Chem.* **2014**, *10*, 1–6.
- (5) The naming of "Togni's reagent 1" and "Togni's reagent 2" are not consistent in different papers. The definition in this paper is consistent with that in ref 13c, one of Togni's early works.

- (6) For allylic trifluoromethylation, see (a) Parsons, A. T.; Buchwald, S. L. *Angew. Chem., Int. Ed.* **2011**, *50*, 9120–9123. (b) Wang, X.; Ye, Y.; Zhang, S.; Feng, J.; Xu, Y.; Zhang, Y.; Wang, J. *J. Am. Chem. Soc.* **2011**, *133*, 16410–16413. (c) Shimizu, R.; Egami, H.; Hamashima, Y.; Sodeoka, M. *Angew. Chem., Int. Ed.* **2012**, *51*, 4577–4580. (d) Mizuta, S.; Galicia-López, O.; Engle, K. M.; Verhoog, S.; Wheelhouse, K.; Rassias, G.; Gouverneur, V. *Chem. - Eur. J.* **2012**, *18*, 8583–8587.

- (7) For olefinic, alkenyl, or aryl trifluoromethylation, see (a) Shimizu, R.; Egami, H.; Nagi, T.; Chae, J.; Hamashima, Y.; Sodeoka, M. *Tetrahedron Lett.* **2010**, *51*, 5947–5949. (b) Parsons, A. T.; Senecal, T. D.; Buchwald, S. L. *Angew. Chem., Int. Ed.* **2012**, *51*, 2947–2950. (c) Mejía, E.; Togni, A. *ACS Catal.* **2012**, *2*, 521–527. (d) Feng, C.; Loh, T.-P. *Chem. Sci.* **2012**, *3*, 3458–3462. (e) Feng, C.; Loh, T.-P. *Angew. Chem., Int. Ed.* **2013**, *52*, 12414–12417. (f) Wang, X.; Ye, Y.; Ji, G.; Xu, Y.; Zhang, S.; Feng, J.; Zhang, Y.; Wang, J. *Org. Lett.* **2013**, *15*, 3730–3733. (g) Ilchenko, N. O.; Janson, P. G.; Szabó, K. J. *Chem. Commun.* **2013**, 49, 6614–6616. (h) Cai, S.; Chen, C.; Sun, Z.; Xi, C. *Chem. Commun.* **2013**, 49, 4552–4554. (i) Pair, E.; Monteiro, N.; Bouyssi, D.; Baudoin, O. *Angew. Chem., Int. Ed.* **2013**, *52*, 5346–5349. (j) Wang, X.-P.; Lin, J.-H.; Zhang, C.-P.; Xiao, J.-C.; Zheng, X. *Beilstein J. Org. Chem.* **2013**, *9*, 2635–2640. (k) Fang, Z.; Ning, Y.; Mi, P.; Liao, P.; Bi, X. *Org. Lett.* **2014**, *16*, 1522–1525. (l) Ji, G.; Wang, X.; Zhang, S.; Xu, Y.; Ye, Y.; Li, M.; Zhang, Y.; Wang, J. *Chem. Commun.* **2014**, *50*, 4361–4363. (m) Prieto, A.; Jeamet, E.; Monteiro, N.; Bouyssi, D.; Baudoin, O. *Org. Lett.* **2014**, *16*, 4770–4773. (n) Gao, P.; Shen, Y.-W.; Fang, R.; Hao, X.-H.; Qiu, Z.-H.; Yang, F.; Yan, X.-B.; Wang, Q.; Gong, X.-J.; Liu, X.-Y.; Liang, Y.-M. *Angew. Chem., Int. Ed.* **2014**, *53*, 7629–7633.

- (8) For oxytrifluoromethylation, see (a) Zhu, R.; Buchwald, S. L. *J. Am. Chem. Soc.* **2012**, *134*, 12462–12465. (b) Li, Y.; Studer, A. *Angew. Chem., Int. Ed.* **2012**, *51*, 8221–8224. (c) Egami, H.; Shimizu, R.; Sodeoka, M. *Tetrahedron Lett.* **2012**, *53*, 5503–5506. (d) Janson, P. G.; Ghoneim, I.; Ilchenko, N. O.; Szabó, K. J. *Org. Lett.* **2012**, *14*, 2882–2885. (e) Zhu, R.; Buchwald, S. L. *Angew. Chem., Int. Ed.* **2013**, *52*, 12655–12658. (f) Lu, D.-F.; Zhu, C.-L.; Xu, H. *Chem. Sci.* **2013**, *4*, 2478–2482. (g) He, Y.-T.; Li, L.-H.; Yang, Y.-F.; Wang, Y.-Q.; Luo, J.-Y.; Liu, X.-Y.; Liang, Y.-M. *Chem. Commun.* **2013**, *49*, 5687–5689. (h) Li, L.; Chen, Q.-Y.; Guo, Y. *J. Org. Chem.* **2014**, *79*, 5145–5152. (i) Xiong, Y.-P.; Wu, M.-Y.; Zhang, X.-Y.; Ma, C.-L.; Huang, L.; Zhao, L.-J.; Tan, B.; Liu, X.-Y. *Org. Lett.* **2014**, *16*, 1000–1003. (j) Egami, H.; Shimizu, R.; Usui, Y.; Sodeoka, M. *J. Fluorine Chem.* **2014**, *167*, 172–178. (k) Egami, H.; Ide, T.; Fujita, M.; Tojo, T.; Hamashima, Y.; Sodeoka, M. *Chem. - Eur. J.* **2014**, *20*, 12061–12065.

- (9) For aminotrifluoromethylation, see (a) Egami, H.; Kawamura, S.; Miyazaki, A.; Sodeoka, M. *Angew. Chem., Int. Ed.* **2013**, *52*, 7841–7844. (b) Lin, J.-S.; Xiong, Y.-P.; Ma, C.-L.; Zhao, L.-J.; Tan, B.; Liu, X.-Y. *Chem. - Eur. J.* **2014**, *20*, 1332–1340. (c) Yang, M.; Wang, W.; Liu, Y.; Feng, L.; Ju, X. *Chin. J. Chem.* **2014**, *32*, 833–837.

- (10) For carbotrifluoromethylation, see (a) Egami, H.; Shimizu, R.; Kawamura, S.; Sodeoka, M. *Angew. Chem., Int. Ed.* **2013**, *52*, 4000–4003. (b) Liu, X.; Xiong, F.; Huang, X.; Xu, L.; Li, P.; Wu, X. *Angew. Chem., Int. Ed.* **2013**, *52*, 6962–6966. (c) Chen, Z.-M.; Bai, W.; Wang, S.-H.; Yang, B.-M.; Tu, Y.-Q.; Zhang, F.-M. *Angew. Chem., Int. Ed.* **2013**, *52*, 9781–9785. (d) Zhang, B.; Mück-Lichtenfeld, C.; Daniliuc, C. G.; Studer, A. *Angew. Chem., Int. Ed.* **2013**, *52*, 10792–10795. (e) Kong, W.; Casimiro, M.; Fuentes, N.; Merino, E.; Nevado, C. *Angew. Chem., Int. Ed.* **2013**, *52*, 13086–13090. (f) Kong, W.; Casimiro, M.; Merino, E.; Nevado, C. *J. Am. Chem. Soc.* **2013**, *135*, 14480–14483. (g) Egami, H.; Shimizu, R.; Usui, Y.; Sodeoka, M. *Chem. Commun.* **2013**, 49, 7346–7348. (h) Ilchenko, N. O.; Janson, P. G.; Szabó, K. J. *J. Org. Chem.* **2013**, *78*, 11087–11091. (i) Egami, H.; Shimizu, R.; Sodeoka, M. *J. Fluorine Chem.* **2013**, *152*, 51–55. (j) He, Y.-T.; Li, L.-H.; Yang, Y.-F.; Zhou, Z.-Z.; Hua, H.-L.; Liu, X.-Y.; Liang, Y.-M. *Org. Lett.* **2014**, *16*, 270–273. (k) Zhang, B.; Studer, A. *Org. Lett.* **2014**, *16*, 1216–1219. (l) He, Y.-T.; Li, L.-H.; Zhou, Z.-Z.; Hua, H.-L.; Qiu, Y.-F.; Liu, X.-Y.; Liang, Y.-M. *Org. Lett.* **2014**, *16*, 3896–3899. (m) Li, Y.; Lu, Y.; Qiu, G.; Deng, Q. *Org. Lett.* **2014**, *16*, 4240–4243.

- (11) For $\text{C}(sp^3)\text{-CF}_3$ bond formation, see (a) Kieltsch, I.; Eisenberger, P.; Togni, A. *Angew. Chem., Int. Ed.* **2007**, *46*, 754–757.

(b) Matošek, V.; Togni, A.; Bizet, V.; Cahard, D. *Org. Lett.* **2011**, *13*, 5762–5765.

(12) For O-CF₃ bond formation, see (a) Stanek, K.; Koller, R.; Togni, A. *J. Org. Chem.* **2008**, *73*, 7678–7685. (b) Koller, R.; Stanek, K.; Stolz, D.; Aardoom, R.; Niedermann, K.; Togni, A. *Angew. Chem., Int. Ed.* **2009**, *48*, 4332–4336. (c) Koller, R.; Huchet, Q.; Battaglia, P.; Welch, J. M.; Togni, A. *Chem. Commun.* **2009**, 5993–5995. (d) Fantasia, S.; Welch, J. M.; Togni, A. *J. Org. Chem.* **2010**, *75*, 1779–1782. (e) Matoušek, V.; Pietrasiak, E.; Sigrist, L.; Czarniecki, B.; Togni, A. *Eur. J. Org. Chem.* **2014**, 3087–3092.

(13) For N-CF₃ bond formation, see (a) Niedermann, K.; Früh, N.; Vinogradova, E.; Wiehn, M. S.; Moreno, A.; Togni, A. *Angew. Chem., Int. Ed.* **2011**, *50*, 1059–1063. (b) Niedermann, K.; Früh, N.; Senn, R.; Czarniecki, B.; Verel, R.; Togni, A. *Angew. Chem., Int. Ed.* **2012**, *51*, 6511–6515. For P-CF₃ bond formation, see (c) Eisenberger, P.; Kieltisch, I.; Armanino, N.; Togni, A. *Chem. Commun.* **2008**, 1575–1577. For S-CF₃ bond formation, see (d) Lin, X.; Wang, G.; Li, H.; Huang, Y.; He, W.; Ye, D.; Huang, K.-W.; Yuan, Y.; Weng, Z. *Tetrahedron* **2013**, *69*, 2628–2632.

(14) (a) Xu, J.; Fu, Y.; Luo, D.-F.; Jiang, Y.-Y.; Xiao, B.; Liu, Z.-J.; Gong, T.-J.; Liu, L. *J. Am. Chem. Soc.* **2011**, *133*, 15300–15303. (b) Xu, J.; Luo, D.-F.; Xiao, B.; Liu, Z.-J.; Gong, T.-J.; Fu, Y.; Liu, L. *Chem. Commun.* **2011**, *47*, 4300–4302. (d) Sala, O.; Lüthi, H. P.; Togni, A. *J. Comput. Chem.* **2014**, *35*, 2122–2131.

(15) (a) Hohenberg, P.; Kohn, W. *Phys. Rev.* **1964**, *136*, B864. (b) Kohn, W.; Sham, L. J. *Phys. Rev.* **1965**, *140*, A1133.

(16) Frisch, M. J.; Trucks, G. W.; Schlegel, H. B.; Scuseria, G. E.; Robb, M. A.; Cheeseman, J. R.; Scalmani, G.; Barone, V.; Mennucci, B.; Petersson, G. A.; Nakatsuji, H.; Caricato, M.; Li, X.; Hratchian, H. P.; Izmaylov, A. F.; Bloino, J.; Zheng, G.; Sonnenberg, J. L.; Hada, M.; Ehara, M.; Toyota, K.; Fukuda, R.; Hasegawa, J.; Ishida, M.; Nakajima, T.; Honda, Y.; Kitao, O.; Nakai, H.; Vreven, T.; Montgomery, A. Jr.; Peralta, J. E.; Ogliaro, F.; Bearpark, M.; Heyd, J. J.; Brothers, E.; Kudin, K. N.; Staroverov, V. N.; Kobayashi, R.; Normand, J.; Raghavachari, K.; Rendell, A.; Burant, J. C.; Iyengar, S. S.; Tomasi, J.; Cossi, M.; Rega, N.; Millam, J. M.; Klene, M.; Knox, J. E.; Cross, J. B.; Bakken, V.; Adamo, C.; Jaramillo, J.; Gomperts, R.; Stratmann, R. E.; Yazyev, O.; Austin, A. J.; Cammi, R.; Pomelli, C.; Ochterski, J. W.; Martin, R. L.; Morokuma, K.; Zakrzewski, V. G.; Voth, G. A.; Salvador, P.; Dannenberg, J. J.; Dapprich, S.; Daniels, A. D.; Farkas, Ö.; Foresman, J. B.; Ortiz, J. V.; Cioslowski, J.; Fox, D. J. *Gaussian 09*, revision A.02; Gaussian, Inc.: Wallingford, CT, 2009.

(17) (a) Becke, A. D. *J. Chem. Phys.* **1993**, *98*, 5648–5652. (b) Lee, C.; Yang, W.; Parr, R. G. *Phys. Rev. B: Condens. Matter Mater. Phys.* **1988**, *37*, 785–789. (c) Vosko, S. H.; Wilk, L.; Nusair, M. *Can. J. Phys.* **1980**, *58*, 1200–1211. (d) Stephens, P. J.; Devlin, F. J.; Chabalowski, C. F.; Frisch, M. J. *J. Phys. Chem.* **1994**, *98*, 11623–11627.

(18) Fuentealba, P.; Preuss, H.; Stoll, H.; Von Szentpály, L. *Chem. Phys. Lett.* **1982**, *89*, 418–422.

(19) Marenich, A. V.; Cramer, C. J.; Truhlar, D. G. *J. Phys. Chem. B* **2009**, *113*, 6378–6396.

(20) For reviews of the two-state reaction, see (a) Armentrout, P. B. *Science* **1991**, *251*, 175–179. (b) Poli, R. *Chem. Rev.* **1996**, *96*, 2135–2204. (c) Schroder, D.; Shaik, S.; Schwarz, H. *Acc. Chem. Res.* **2000**, *33*, 139–145. (d) Poli, R.; Harvey, J. N. *Chem. Soc. Rev.* **2003**, *32*, 1–8. (e) Schwarz, H. *Int. J. Mass Spectrom.* **2004**, *237*, 75–105. (f) Harvey, J. N. *Phys. Chem. Chem. Phys.* **2007**, *9*, 331–343. (g) Besora, M.; Carreón-Macedo, J. L.; Cimas, A.; Harvey, J. N. *Adv. Inorg. Chem.* **2009**, *61*, 573–623. (h) Yarkony, D. R. *Chem. Rev.* **2012**, *112*, 481–498. (i) Marian, C. M. *WIREs Comput. Mol. Sci.* **2012**, *2*, 187–203. (j) Harvey, J. N. *WIREs Comput. Mol. Sci.* **2014**, *4*, 1–14.

(21) Selected references for MECP locating technique (a) Koga, N.; Morokuma, K. *Chem. Phys. Lett.* **1985**, *119*, 371–374. (b) Bearpark, M. J.; Robb, M. A.; Schlegel, H. B. *Chem. Phys. Lett.* **1994**, *223*, 269–274. (c) Harvey, J. N.; Aschi, M.; Schwarz, H.; Koch, W. *Theor. Chem. Acc.* **1998**, *99*, 95–99. (d) Chachiyo, T.; Rodriguez, J. H. *J. Chem. Phys.* **2005**, *123*, 094711. (e) Liu, K.; Li, Y.; Su, J.; Wang, B. *J. Comput. Chem.* **2014**, *35*, 703–710.

(22) Selected examples for using B3LYP in TSR calculation (a) Yoshizawa, K.; Shiota, Y.; Yamabe, T. *J. Am. Chem. Soc.* **1999**, *121*, 147–153. (b) Yoshizawa, K.; Shiota, Y.; Yamabe, T. *J. Chem. Phys.* **1999**, *111*, 538–545. (c) Carreón-Macedo, J.-L.; Harvey, J. N. *J. Am. Chem. Soc.* **2004**, *126*, 5789–5797. (d) Werz, D. B.; Klatt, G.; Raskatov, J. A.; Köppel, H.; Gleiter, R. *Organometallics* **2009**, *28*, 1675–1682. (e) Dahy, A. A.; Koga, N. *J. Organomet. Chem.* **2010**, *695*, 2240–2250. (f) Benito-Garagorri, D.; Lagoja, I.; Veiros, L. F.; Kirchner, K. A. *Dalton Trans.* **2011**, *40*, 4778–4792. (g) Manner, V. W.; Lindsay, A. D.; Mader, E. A.; Harvey, J. N.; Mayer, J. M. *Chem. Sci.* **2012**, *3*, 230–243. (h) Lv, L.; Wang, X.; Zhu, Y.; Liu, X.; Wang, Y. *Sci. China: Chem.* **2012**, *55*, 158–166. (i) Huang, S.-P.; Shiota, Y.; Yoshizawa, K. *Dalton Trans.* **2013**, *42*, 1011–1023. (j) Dai, F.; Yap, G. P. A.; Theopold, K. H. *J. Am. Chem. Soc.* **2013**, *135*, 16774–16776. (k) Ling, L.; Chen, J.; Song, J.; Zhang, Y.; Li, X.; Song, L.; Shi, F.; Li, Y.; Wu, C. *Org. Biomol. Chem.* **2013**, *11*, 3894–3902.

(23) Selected references for using B3LYP in broken symmetry state calculation (a) Bendikov, M.; Duong, H. M.; Starkey, K.; Houk, K. N.; Carter, E. A.; Wudl, F. *J. Am. Chem. Soc.* **2004**, *126*, 7416–7417. (b) et al. *J. Am. Chem. Soc.* **2004**, *126*, 10493.10.1021/ja0457258 (c) Blusch, L. K.; Craigo, K. E.; Martin-Diaconescu, V.; McQuarters, A. B.; Bill, E.; Decheert, S.; DeBeer, S.; Lehnert, N.; Meyer, F. *J. Am. Chem. Soc.* **2013**, *135*, 13892–13899. (d) Yao, Z.; Yu, Z. *J. Am. Chem. Soc.* **2011**, *133*, 10864–10877.

(24) See Supporting Information.

(25) Reed, A. E.; Curtiss, L. A.; Weinhold, F. *Chem. Rev.* **1988**, *88*, 899–926.

(26) In many cases, the *closed-shell-singlet/singlet-diradical* MECPs are more favorable than the *closed-shell-singlet/triplet* MECPs. Thus in the following sections, only the former are given.

(27) Davies, D. L.; Donald, S. M. A.; Macgregor, S. A. *J. Am. Chem. Soc.* **2005**, *127*, 13754–13755.

(28) (a) Röck, M.; Schmittel, M. *J. Chem. Soc., Chem. Commun.* **1993**, 1739–1741. (b) Connelly, N. G.; Geiger, W. E. *Chem. Rev.* **1996**, *96*, 877–910. (c) Jahn, U.; Hartmann, P.; Kaasalainen, E. *Org. Lett.* **2004**, *6*, 257–260.

(29) (a) Iseki, K.; Nagai, T.; Kobayashi, Y. *Tetrahedron Lett.* **1993**, *34*, 2169–2170. (b) Iseki, K.; Nagai, T.; Kobayashi, Y. *Tetrahedron: Asymmetry* **1994**, *5*, 961–974. (c) Iseki, K.; Takahashi, M.; Asada, D.; Nagai, T.; Kobayashi, Y. *J. Fluorine Chem.* **1995**, *74*, 269–271. (d) Tomita, Y.; Ichikawa, Y.; Itoh, Y.; Kawada, K.; Mikami, K. *Tetrahedron Lett.* **2007**, *48*, 8922–8925.